IN2P3 Prospectives 2020
GT05 Physique de l'inflation et énergie noire

Cosmic Inflation: Observation from the Ground-Based CMB Polarization Experiments

Porteur: Josquin Errard [a,1]

Antony Banday,[d] **Dominic Beck,**[a] **Hamza El Bouhargani,**[a] **Josquin Errard,**[a] **Ken Ganga,**[a] **Yannick Giraud-Héraud,**[a] **Jean-Christophe Hamilton,**[a] **Sophie Henrot-Versillé,**[b] **Baptiste Jost,**[a] **Elias Kiritsis,**[a] **Clément Leloup,**[a] **Thibaut Louis,**[b] **Juan Macìas-Pérez**[c] **Ludovic Montier,**[d] **Baptiste Mot,**[d] **Francesco Nitti,**[a] **Guillaume Patanchon,**[a] **Vincent Pelgrims,**[f] **Michel Piat**[a] **Radek Stompor,**[a] **Bartjan van Tent,**[e] **Matthieu Tristram,**[b] **Vincent Vennin,**[a] **Clara Vergès**[a]

[a]AstroParticule et Cosmologie, Univ Paris Diderot, CNRS/IN2P3, CEA/Irfu, Obs de Paris, Sorbonne Paris Cité, France

[b]Laboratoire de l'Accélérateur Linéaire, Univ. Paris-Sud, CNRS/IN2P3, Université Paris-Saclay, Orsay, France

[c]Laboratoire de Physique Subatomique et Cosmologie, Université Grenoble-Alpes, CNRS/IN2P3, 53, rue des Martyrs, 38026 Grenoble Cedex, France

[d]CNRS, IRAP, 9 Av. colonel Roche, BP 44346, F-31028 Toulouse cedex 4, France

[e]Laboratoire de Physique Théorique, Université Paris-Sud 11 CNRS, Bâtiment 210, 91405 Orsay, France

[f]Institute of Astrophysics, Foundation for Research and Technology-Hellas, GR-71110 Heraklion, Greece,
Department of Physics, Univ. of Crete, GR-70013 Heraklion, Greece
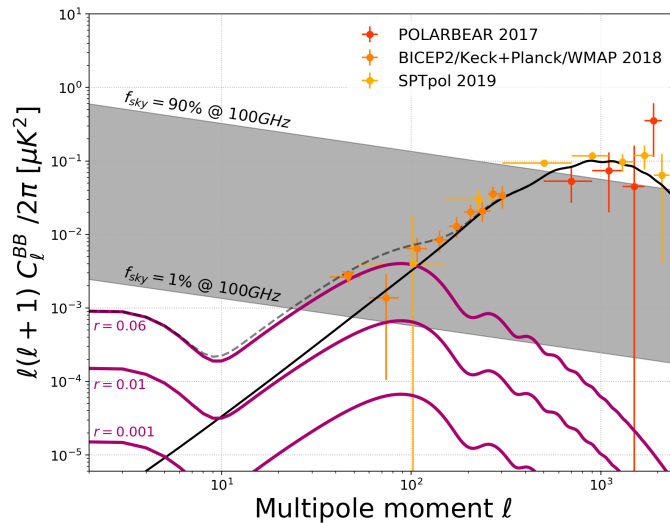
Figure 1. Angular power spectrum of B-modes, C_ℓ^{BB}, with direct measurements coming from POLARBEAR [1], BICEP-Keck Array with Planck / WMAP [2] and SPTPol [3], as well as the expected foregrounds power (gray band) at 100GHz for the cleanest 1% of the sky to a 90% galactic mask. We outline the theoretical primordial BB curves, in purple, for a tensor-to-scalar ratio of $r = 0.001$, 0.01 and 0.06 (current upper limit at 95% C.L.). Contribution from gravitational lensing to B-modes is shown as the solid black line.

1 Introduction: observables from inflation

The companion paper *Cosmic Inflation I: theory* [4] summarizes how the inflation scenario [5–8] produces a background of gravitational waves propagating through the primordial, hot and dense plasma [9]. Then, through Thomson scattering, the CMB light gets polarized through quadrupolar anisotropies induced by scalar and tensor perturbations [10]. The produced patterns of polarization, which are nowadays visible on the last scattering surface, are decomposed in a mathematical basis allowing us to distinguish both perturbations. The so-called E-modes, which are rotational free polarization patterns, are generated by both scalar and tensor perturbations, whereas the B-modes, which are gradient free patterns, can only be generated by tensor perturbations.
This is true onto the last scattering surface, in the absence of symmetry breaking mechanisms such as cosmic birefringence or primordial magnetic fields, and without secondary anisotropies (e.g. gravitational lensing), as discussed in section 2.

The best observational channel to look for primordial gravitational waves generated by cosmic inflation is through the B-modes signal at the largest angular scales. In particular, the CMB community is putting significant efforts in constraining the tensor-to-scalar ratio r, involved in the following decomposition of the observed B-modes angular

---

[1]josquin@apc.in2p3.fr

power spectrum:

$$C_\ell^{\mathrm{BB,\,obs}} = r \times C_\ell^{\mathrm{BB,\,prim}}(r=1) + C_\ell^{\mathrm{BB,\,lens}} + C_\ell^{\mathrm{BB,\,noise}} + C_\ell^{\mathrm{BB,\,fgs}} \tag{1.1}$$

where the two first terms in the right hand side correspond to the primordial gravitational waves and the gravitational lensing parts, and are illustrated in Fig. 1. $C_\ell^{\mathrm{BB,\,noise}}$ corresponds to the instrumental noise, usually propagated through the foregrounds cleaning. And $C_\ell^{\mathrm{BB,\,fgs}}$ is the galactic foregrounds either measured at a given frequency, or left-over residuals after a cleaning of the foregrounds.

From Eq. 1.1, one can express the simple Fisher uncertainty on $r = 0$ as

$$\sigma(r=0) \sim \frac{1}{\sqrt{\frac{\mathrm{f_{sky}}}{2} \sum_{\ell=\ell_{\min}}^{\ell_{\max}} (2\ell+1) \left(\frac{C_\ell^{\mathrm{BB,\,prim}}(r=1)}{C_\ell^{\mathrm{BB,\,lens}} + C_\ell^{\mathrm{BB,\,noise}} + C_\ell^{\mathrm{BB,\,fgs}}} \right)^2}} \tag{1.2}$$

From Eq. 1.2, one can notice that the sensitivity of a given instrument to r will depend on the fraction of observed sky, $\mathrm{f_{sky}}$, on the observed multipoles ℓ, as well as on the amplitude of lensing B-modes, noise and foregrounds residuals. In particular, given the red-spectrum of primordial B-modes, cf. Fig. 1, Eq. 1.2 shows the importance of achieving the lowest $\ell_{\min}$ possible in order to lower $\sigma(r)$. Assuming that foregrounds are negligible in front of the noise and lensing B-modes, and that $C_\ell^{\mathrm{BB,\,lens}} \sim \mathrm{A_{lens}} \times (5\,\mu\mathrm{K} - \mathrm{arcmin})^2$ and $C_\ell^{\mathrm{BB,\,noise}} \sim \mathrm{NET}^2 \mathrm{f_{sky}}/(\mathrm{N_{det}T_{obs}})$, Eq. 1.2 can be approximated as

$$\sigma(r=0) \propto \frac{(25\,[(\mu\mathrm{K} - \mathrm{arcmin})^2]) \times \mathrm{A_{lens}} + \frac{(\mathrm{NET}\,[\mu\mathrm{K}\sqrt{\mathrm{s}}])^2 (\mathrm{f_{sky}}\,[\mathrm{arcmin}^2])}{(\mathrm{N_{det}T_{obs}}\,[\mathrm{s}])}}{\sqrt{\mathrm{f_{sky}}\,[\mathrm{arcmin}^2]}} \tag{1.3}$$

where the Noise Equivalent Temperature (NET) is given for one detector. Eq. 1.3 shows why focusing on a small patch ($\mathrm{f_{sky}} \ll 4\pi$) with many detectors-time ($\mathrm{N_{det}} \times \mathrm{T_{obs}} \gg 1\mathrm{s}$) is the observational strategy adopted by most of the current projects to reach $r \leq 0.01$ [11, 12]. With a decreasing noise, sensitivity to r starts being limited by cosmic-variance from lensing B-modes: there are techniques to reduce their contribution, see paragraph 2.3.

The choice of B-modes is due to the fact that, with a similar formalism as in Eq. 1.2, we can show that a perfect measurement of temperature and E-modes anisotropies would only be able to reject $r = 0$ with a conditional $\sigma(r=0) \sim \mathcal{O}(0.02)$ cosmic-variance uncertainty. This is roughly at the same level as the current lowest upper limit, $r < 0.06$ at 95% confidence level determined by the combination of BICEP2-Keck Array, WMAP and Planck data sets [2].

The proposed goal for the 2020-2030 generation CMB polarization observatories is to probe inflationary models with $r \sim 0.001$ gravitational waves amplitude – this is a typical prediction from Starobinski model [5]. In practice, as already suggested by Eq. 1.2, reaching the low amplitude of the corresponding primordial B-modes requires to overcome several challenges – observational, technological and related to data analysis.
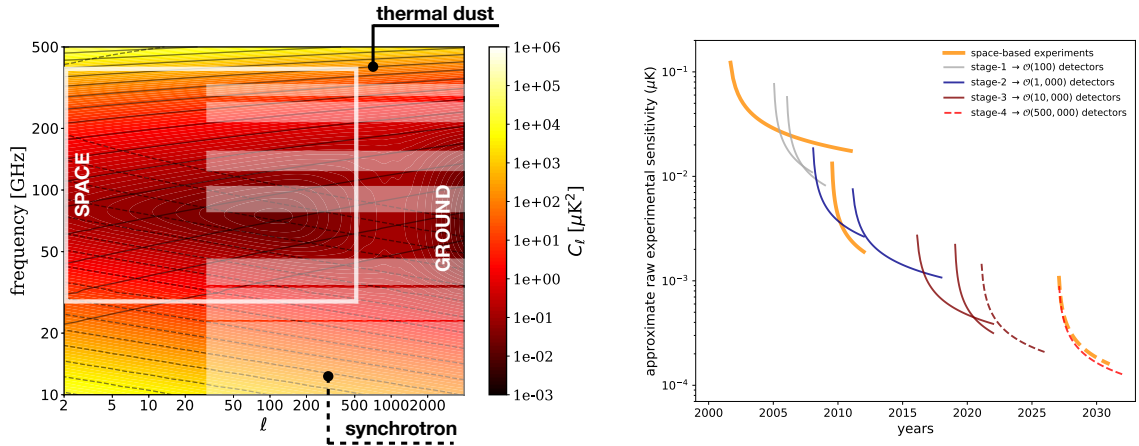
Figure 2. *Left panel*: amplitude of the polarized dust (solid black contours) and synchrotron (dash black contours) angular power spectrum as a function of multipoles ℓ (x-axis)) and frequency of observation (y-axis). These are the estimated power for f_{sky} = 60% [16, 17]. We add the typical observation bands for a space mission (solid white frame on the left) and ground-based observatory (white transparent boxes on the right). *Right panel*: evolution of typical instrumental sensitivity through the years, through the increase of the number of detectors, cf. the $NET/\sqrt{N_{det}T_{obs}}$ term in Eq. 1.3. Modified from CMB-S4 Science Book [18]. It assumes a 10% efficiency for ground-based experiments. Dash curves correspond to upcoming/planed projects.

2 Observational, technological and analysis challenges

2.1 Instrumental sensitivity

In the race to r, instrumental sensitivity is one of the most critical parameters: measuring the power of lensing B-modes with a signal-to-noise of 1 typically requires having 1000 detectors observing 1% of the sky for 1 effective year, under the typical atmospheric conditions at 5,000m in the Atacama desert in Chile.

Today, focal planes of ground-based instruments, so-called Stage-3 projects, typically use $\mathcal{O}(10^4)$ photon-noise limited detectors. Yet, in this era of highly sensitive focal planes, low-frequency noises have to be controlled and possibly rejected as they directly reduce sensitivity on the largest angular scales where the B-modes signal is the strongest ($C_\ell^{BB,\,noise}$ in Eq. 1.2 typically becomes $\propto 1/\ell$, [13]). To overcome this problem, several collaborations [14, 15] have opted for continuously rotating half-wave plates (HWP), an optical element which modulates the incoming polarized sky signal to frequencies higher than the contaminated low-frequency noise. But slowly-varying contaminants such as atmosphere loading, ground-pickups, etc. remain among the main limiting factors for current and up-coming B-modes measurements.

2.2 Galactic foregrounds

As suggested in Fig. 1, the current most sensitive measurements on the largest scales are limited by galactic foregrounds – mainly induced by the thermal emission from galactic

dust and by synchrotron radiation. This is also shown in the left panel of Fig. 2, where the angular power of polarized dust and synchrotron are depicted as a function of frequency, following Planck results [16, 17]. The lowest foregrounds amplitude is typically achieved around 70GHz, but does not allow for any sensible detection of primordial CMB B-modes below $r \sim 0.1$ [19].

The new generation of CMB polarization observatories has therefore to characterize the sky signals at different wavelengths in order to distinguish the CMB black body from other astrophysical emissions. Fig. 2 shows the complementarity of ground and space projects. Although space can probe a continuous frequency spectrum without being limited by atmosphere, and constrain the lowest multipoles through an observation of the entire sky, it is usually limited by the size of its optics (and has therefore a limited resolution, and cannot make sensible measurements at the lowest frequencies). Ground projects, on the other hand, can observe in $\sim 6 - 7$ frequency bands, focusing on a small fraction of sky and on B-modes power around the recombination bump ($\ell \sim 80$). Exchange of information between these two types of observation are and will be very fruitful.

The understanding and removal of spurious emissions is called component separation, and is a very active research area. The precision of the developed algorithms is likely to be soon limited by our ability to model and understand the interstellar physics. The simple fact that dust and synchrotron SEDs are spatially varying across the observed sky increases the required algorithmic degrees of freedom that data analysts have to adjust, hence driving the final sensitivity to characterize the recovered B-modes signal [20]. The combination of such ground-based data sets with specific foregrounds monitors (e.g. coming from a space mission [21] or from low-frequency measurements from the ground [22–24] and high-frequency from balloons [25–27]) could be of tremendous help to succeed this challenge.

2.3 Gravitational lensing

B-modes generated by gravitational lensing are dominant at sub-degree scales, as can be seen in Fig. 1. New and upcoming instruments reaching noise levels of ≤ 5 μK-arcmin will be limited by the lensing-induced cosmic variance in their detection of the primordial gravitational wave signal. For a typical ground-based instrument observing multipoles $\ell \geq 30$, the lensing-limited sensitivity on r is $\sigma(r = 0) \sim 0.002$ [12]. Achieving lower sensitivities requires either a measurement of the largest scales down to $\ell = 2$, as planned for space missions [21], or the removal of the variance caused by gravitational lensing. The latter goes under the name of delensing and can be achieved by including extra information from high resolution measurements of E-modes combined with one or more tracers of large scale structure in the Universe, i.e. from high resolution CMB data itself (internal delensing) [28], or from CIB or optical weak lensing surveys (external delensing) [29]. A first demonstration of feasibility of internal delensing in the relevant noise regime has been reported in [30].

2.4 Instrumental systematics

The mitigation of systematic effects in data, originating from instrumental effect modeling imperfections or uncertainties is crucial for the unbiased estimation of the cosmological signal. Those effects include detector cross-talk, detector correlated noise (either intrinsic of from the atmosphere), instrumental polarization from the optical elements, sidelobe pickups, beam and gain mismatches (in case no HWP is used). The coupling of effects is also creating artefacts potentially limiting the correction: this is the case of the leakage of the large atmospheric signal to the polarization estimation induced by the HWP in presence of detector non-linearity, although the use of a HWP limits many systematic effects by allowing quasi-instantaneous estimation of the polarization signal. Most important effects induce a leakage from intensity to polarization and a mixing between E and B components.

Standard techniques use templates of the effects based on intensity maps previously measured by experiment like the Planck satellite, and perform a so called de-projection which consists in removing the contribution of the leakage to polarization map estimates. Those techniques are usually combined with a high-pass filtering of the timestreams to remove contribution (which is mostly anisotropic on the sky due to the particularity of the scanning strategy) at large scales in the maps. Advanced methods preform a joint analysis of polarization maps and template-based parametric estimation/correction of systematic effects.

In particular, high fidelity modeling of systematic effects is necessary to assess their impact on data. Understanding how instrumental parameters play a role, for example in the case of intensity-to-polarization leakage, allows to account for these effects in the data analysis process, and to correct for them without using external data. Moreover, in the context of multi-frequency experiments which are requiring advanced component separation techniques, it is crucial to understand and model the impact of frequency- and component-dependent effects, such as the ones induced by the HWP.

2.5 Analysis of large data sets

The ever more increasing sensitivities, right panel of Fig. 2, unavoidably leads to an exponential growth of the volumes of data. The size of the full raw data sets that we need to process is soon expected to reach the Petabytes scale in the forthcoming CMB experiments. Concurrently, increasingly more complex data models are required to take into account spurious signals and systematic effects in our analyses, which typically entails more involved computations. For such processing to be efficient, our numerical tools need to be not only optimized in terms of the number of floating point operations (FLOPS) but also in terms of their implementation with regards to the hardware architecture of modern supercomputers which are used for these processings [31]. Typically, reducing the raw CMB timestreams into sky maps will require the usage of $\mathcal{O}(10^5)$ processors given the expected size of the future data sets. On one hand, such a procedure will involve heavy communication, which may hinder the scalability of our current algorithms. On the other hand, the size of the data is such that we may also start to be limited by memory. To address these problems, we may need to redesign our data
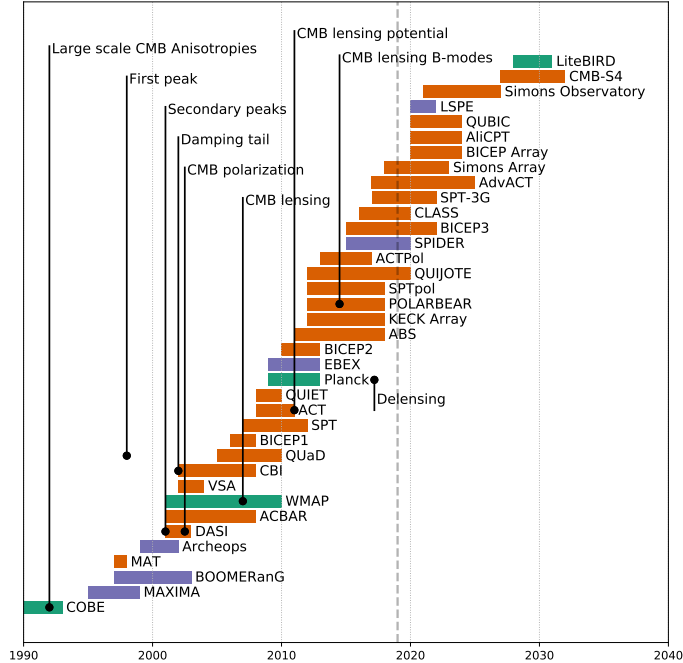
Figure 3. Deployment of ground, balloon and space CMB instruments in the past 30 years.

distribution schemes [32], and the implementation of our algorithms to minimize the number of communication instances, and make efficient use of memory, for example by computing elements of the data in a piecewise manner on the fly, instead of loading the full data on memory at once.

3   On-going and upcoming ground-based observatories

Overcoming challenges listed above require new instrumental designs, involving low-noise multi-frequency detectors, sensitive to polarization. Designs are also driven by the control of systematic effects, mainly regarding the thermal stability of the instrument, high-precision calibration of the optical/frequential response as well as a strong rejection of spurious signals coming from the telescopes' surroundings. [12] showed that complementary multi-frequency observations with dedicated large- and small-angular scale observation campaign was the most cost-effective program to reach primordial B-modes from the ground, along with achieving the science goals related to the formation of large scale structures. This is for instance the chosen design for the Simons Observatory, with a Large Aperture Telescope complementing an array of B-modes-focused Small Aperture Telescopes [33]. Several frequency bands would be used to clean galactic foregrounds, see paragraph 2.2, and a high resolution CMB campaign would provide a sensitive measurement of the lensing potential, used for delensing, see paragraph 2.3.

The right panel of Fig 2 shows the evolution of instrumental sensitivities through the years. The use of larger focal planes translates into a decrease of the instantaneous instrumental sensitivity, $\propto \mathrm{NET}/\sqrt{\mathrm{T_{obs} \times N_{det}}}$. This addresses the challenge associated to sensitivity, described in paragraph 2.1, in the context of photon-noise limited detectors [34]. In particular, the goal of current Stage-3 and future Stage-4 projects is to reach noise levels after component separation, $C_\ell^{\mathrm{BB,\,noise}}$ in Eq. 1.2, which are lower than lensing B-modes, and foregrounds residuals, $C_\ell^{\mathrm{BB,\,foregrounds}}$, which are much lower than the targeted primordial B-modes.

Fig. 3 summarizes the evolution of past, current and future ground-based, balloon-borne and space observatories. After first detection of the lensing peak, the on-going race to B-modes focuses on the characterization of the recombination B-modes bump, around $\ell \sim 80$, which seems to be at reach with sub-orbital projects, when they focus their sensitivity on a small fraction of the sky, typically f_{sky} = 1-10% allowing them to observe low-foregrounds regions, in regions distant from the galactic plane. Characterization and mitigation of astrophysical and instrumental systematic effects, by definition unknown, will be key to their success.

A complementary approach is proposed by the LiteBIRD design, as detailed in the companion paper *Cosmic Inflation III: observations from space, LiteBIRD* [21], with a full-sky coverage in 15 frequency bands, probing both reionization and recombination bumps with high sensitivity.

References

[1] POLARBEAR Collaboration, P. A. R. Ade, M. Aguilar, Y. Akiba, K. Arnold, C. Baccigalupi et al., *A Measurement of the Cosmic Microwave Background B-mode Polarization Power Spectrum at Subdegree Scales from Two Years of polarbear Data*, **848** (Oct., 2017) 121, [1705.02907].

[2] The BICEP/Keck Collaboration, :, P. A. R. Ade, Z. Ahmed, R. W. Aikin, K. D. Alexander et al., *Measurements of Degree-Scale B-mode Polarization with the BICEP/Keck Experiments at South Pole*, ArXiv e-prints (July, 2018) , [1807.02199].

[3] J. T. Sayre, C. L. Reichardt, J. W. Henning, P. A. R. Ade, A. J. Anderson, J. E. Austermann et al., *Measurements of B-mode Polarization of the Cosmic Microwave Background from 500 Square Degrees of SPTpol Data*, arXiv e-prints (Oct., 2019) , [1910.05748].

[4] V. V. *et al.*, *GT05 IN2P3 prospectives: Cosmic inflation: theory*, .

[5] A. A. Starobinsky, *Spectrum of relict gravitational radiation and the early state of the universe*, JETP Lett. **30** (1979) 682–685.

[6] A. H. Guth, *The Inflationary Universe: A Possible Solution to the Horizon and Flatness Problems*, Phys. Rev. **D23** (1981) 347–356.

[7] A. D. Linde, *A New Inflationary Universe Scenario: A Possible Solution of the Horizon, Flatness, Homogeneity, Isotropy and Primordial Monopole Problems*, Phys. Lett. **108B** (1982) 389–393.

[8] A. Albrecht and P. J. Steinhardt, *Cosmology for grand unified theories with radiatively induced symmetry breaking*, *Physical Review Letters* **48** (Apr., 1982) 1220–1223.

[9] S. Henrot-Versille et al., *Improved constraint on the primordial gravitational-wave density using recent cosmological data and its impact on cosmic string models*, *Class. Quant. Grav.* **32** (2015) 045003, [1408.5299].

[10] W. Hu and M. White, *A CMB polarization primer*, **2** (Oct, 1997) 323–344, [astro-ph/9706147].

[11] W. L. K. Wu, J. Errard, C. Dvorkin, C. L. Kuo, A. T. Lee, P. McDonald et al., *A Guide to Designing Future Ground-based Cosmic Microwave Background Experiments*, **788** (June, 2014) 138, [1402.4108].

[12] D. Barron, Y. Chinone, A. Kusaka, J. Borril, J. Errard, S. Feeney et al., *Optimization study for the experimental configuration of CMB-S4*, **2** (Feb., 2018) 009, [1702.07467].

[13] The Simons Observatory Collaboration, P. Ade, J. Aguirre, Z. Ahmed, S. Aiola, A. Ali et al., *The Simons Observatory: Science goals and forecasts*, *ArXiv e-prints* (Aug., 2018) , [1808.07445].

[14] J. Didier, A. D. Miller, D. Araujo, F. Aubin, C. Geach, B. Johnson et al., *Intensity-Coupled-Polarization in Instruments with a Continuously Rotating Half-Wave Plate*, *arXiv e-prints* (Nov., 2017) , [1711.01314].

[15] S. Adachi, M. A. O. Aguilar Faúndez, K. Arnold, C. Baccigalupi, D. Barron, D. Beck et al., *A Measurement of the Degree Scale CMB B-mode Angular Power Spectrum with POLARBEAR*, *arXiv e-prints* (Oct., 2019) , [1910.02608].

[16] Planck Collaboration, P. A. R. Ade, N. Aghanim, M. I. R. Alves, M. Arnaud, M. Ashdown et al., *Planck 2015 results. XXV. Diffuse low-frequency Galactic foregrounds*, **594** (Sept., 2016) A25, [1506.06660].

[17] Planck Collaboration, R. Adam, P. A. R. Ade, N. Aghanim, M. Arnaud, J. Aumont et al., *Planck intermediate results. XXX. The angular power spectrum of polarized dust emission at intermediate and high Galactic latitudes*, **586** (Feb., 2016) A133, [1409.5738].

[18] K. N. Abazajian, P. Adshead, Z. Ahmed, S. W. Allen, D. Alonso, K. S. Arnold et al., *CMB-S4 Science Book, First Edition*, *ArXiv e-prints* (Oct., 2016) , [1610.02743].

[19] N. Krachmalnicoff, C. Baccigalupi, J. Aumont, M. Bersanelli and A. Mennella, *Characterization of foreground emission on degree angular scales for CMB B-mode observations . Thermal dust and synchrotron signal from Planck and WMAP data*, **588** (Apr., 2016) A65.

[20] J. Errard and R. Stompor, *Characterizing bias on large scale CMB B-modes after Galactic foregrounds cleaning*, **99** (Feb., 2019) 043529, [1811.00479].

[21] M. T. *et al*, *GT05 IN2P3 prospectives: Cosmic inflation: observations from space, LiteBIRD*, .

[22] N. Krachmalnicoff, E. Carretti, C. Baccigalupi, G. Bernardi, S. Brown, B. M. Gaensler et al., *S-PASS view of polarized Galactic synchrotron at 2.3 GHz as a contaminant to CMB observations*, **618** (Oct., 2018) A166, [1802.01145].

[23] M. E. Jones, A. C. Taylor, M. Aich, C. J. Copley, H. C. Chiang, R. J. Davis et al., *The C-Band All-Sky Survey (C-BASS): design and capabilities*, **480** (Nov., 2018) 3224–3242, [1805.04490].

[24] F. Poidevin, J. A. Rubino-Martin, R. Genova-Santos, R. Rebolo, M. Aguiar, F. Gomez-Renasco et al., *The QUIJOTE Experiment: Prospects for CMB B-MODE polarization detection and foregrounds characterization*, arXiv e-prints (Feb., 2018) , [1802.04594].

[25] N. Gandilo and BLAST-Pol Collaboration, *The Balloon-borne Large Aperture Submillimeter Telescope for Polarimetry (BLAST-Pol): Instrument and 2010 Science Campaign*, in *American Astronomical Society Meeting Abstracts #219*, vol. 219 of *American Astronomical Society Meeting Abstracts*, p. 422.29, Jan., 2012.

[26] S. Hanany, "EBEX-IDS: A Balloon-Borne Experiment to Observe and Separate Galactic Dust from Cosmic Inflation Signals." NASA APRA Proposal, 2015.

[27] J. Aumont, *Measuring the diffuse FIR polarized dust emission with PILOT for the quest of CMB B-modes*, in *42nd COSPAR Scientific Assembly*, vol. 42 of *COSPAR Meeting*, pp. E1.2–18–18, July, 2018.

[28] J. Carron, A. Lewis and A. Challinor, *Internal delensing of Planck CMB temperature and polarization*, **5** (May, 2017) 035, [1701.01712].

[29] A. Manzotti, K. T. Story, W. L. K. Wu, J. E. Austermann, J. A. Beall, A. N. Bender et al., *CMB Polarization B-mode Delensing with SPTpol and Herschel*, **846** (Sept., 2017) 45, [1701.04396].

[30] S. Adachi, M. A. O. Aguilar Faúndez, Y. Akiba, A. Ali, K. Arnold, C. Baccigalupi et al., *Internal delensing of cosmic microwave background polarization B-modes with the POLARBEAR experiment*, arXiv e-prints (Sept., 2019) , [1909.13832].

[31] "Big Bang from Big Data of the Cosmic Microwave Background." http://b3dcmb.in2p3.fr/, Oct., 2019.

[32] C. M. Cantalupo, J. D. Borrill, A. H. Jaffe, T. S. Kisner and R. Stompor, *MADmap: A Massively Parallel Maximum Likelihood Cosmic Microwave Background Map-maker*, **187** (Mar., 2010) 212–227, [0906.1775].

[33] T. L. *et al*, *GT05 IN2P3 prospectives: Fundamental physics from high resolution CMB experiments*, .

[34] M. P. *et al*, *GT05 IN2P3 prospectives: CMB detectors*, .